IOP Conf. Series: Materials Science and Engineering **1344** (2026) 012102 doi:10.1088/1757-899X/1344/1/012102

Process Simulation and Techno-Economic Assessment of Hydrogen Liquefaction Plants with Integrated Ortho-Para Conversion

Laura Stops[1], **Benjamin Kanz**[1,2], **Khang Do**[1], **Sebastian Rehfeldt**[1] **and Harald Klein**[1]

[1]Technical University of Munich, TUM School of Engineering and Design, Department of Energy and Process Engineering, Institute of Plant and Process Technology, Garching, Germany
[2]TUMCREATE Ltd., 1 Create Way, Singapore

E-mail: laura.stops@tum.de

Abstract. Hydrogen liquefaction plants are a key component of liquid hydrogen supply chains. However, to meet future hydrogen demands for climate-friendly mobility, a significant scale-up is necessary. This study aims to provide a deeper understanding of hydrogen liquefaction plants by presenting process simulations of smaller- and large-scale plants using UniSim® Design. The process simulations accurately integrate the conversion of orthohydrogen to parahydrogen taking place continuously within the heat exchanger channels, along with the associated conversion heat. A techno-economic analysis evaluates the cost-effectiveness and energy efficiency of the processes. The results, which are validated against literature data, indicate that CAPEX and OPEX contribute equally to the overall liquefaction costs, with heat exchangers and compressors identified as the main cost drivers. A significant reduction in specific CAPEX and specific energy consumption is observed with increasing plant size, influenced by economy of scale and precooling technology. By integrating process simulation with techno-economic evaluation, this study provides valuable insights into the performance and specific costs of hydrogen liquefaction plants.

1 Introduction

Resulting from the rising need for CO_2-emission-free solutions in the transportation sector, liquid hydrogen (LH_2) emerges as a promising fuel of the future. Especially in energy-intensive applications, such as aircraft, the application of LH_2 is being thoroughly studied in recent years (e.g., [1]).

In the joint project "HyNEAT", LH_2 supply networks for airports are being examined. The project investigates how these LH_2 networks could look like in 2050, as well as the transition pathways towards a hydrogen powered aviation sector. Hydrogen liquefaction plants are key within such supply networks as they come with high investment costs and high energy requirements. However, as LH_2 is just emerging as a climate-friendly fuel and as there are few current applications, today's liquefaction capacity is rather low. As such, only approximately 380 tonnes per day (tpd) of hydrogen were liquefied globally in 2021 [2]. Therefore, a significant upscale is required considering that projected demands for liquid hydrogen in aviation alone are several magnitudes larger [3].

This paper studies the techno-economics of hydrogen liquefaction plants based on process simulation. The following sections first introduce the simulation of selected processes with UniSim® Design and the integration of the ortho-para conversion. Then, the methodology of the techno-economic assessment is presented and the results are discussed and compared to the literature.

Content from this work may be used under the terms of the Creative Commons Attribution 4.0 licence. Any further distribution of this work must maintain attribution to the author(s) and the title of the work, journal citation and DOI.
Published under licence by IOP Publishing Ltd

2 Methodology

Typically, a hydrogen liquefaction plant follows the setup in Figure 1. First, gaseous hydrogen (GH_2) is precooled, e.g., using liquid nitrogen (LN_2) which is either released to the environment, as shown in Figure 2, or recycled. Then, the hydrogen is purified in an adsorber at 80 K to 100 K before it enters the cryogenic refrigeration and liquefaction section, where it is cooled and liquefied in plate-fin heat exchangers using a cryogenic refrigeration cycle and a Joule-Thomson valve. For refrigeration, in this paper, hydrogen Claude cycles are applied. Thereby the refrigerant, which is also hydrogen, is compressed at ambient temperatures. The compression heat is dissipated using cooling water. Later in the cycle, the cold temperatures are achieved by expansion in turbo expanders and another Joule-Thomson valve.

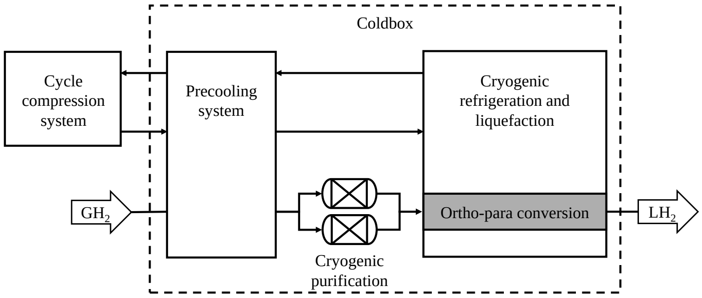

Figure 1: Simplified flowsheet of a typical hydrogen liquefaction plant, adapted from CARDELLA 2018 [4]

To minimize heat in-leak, the cold sections of the plant are placed within a coldbox. Further, in the cryogenic section, the conversion of orthohydrogen to parahydrogen takes place within catalyst-filled heat exchanger channels, which will be discussed in section 2.2.

2.1 Process Simulation

In this paper, hydrogen liquefaction plants are simulated and assessed. As a typical process of relatively smaller scale, the flowsheet in Figure 2 based on the 5 tpd plant by OHLIG & DECKER 2024 [5] is chosen.

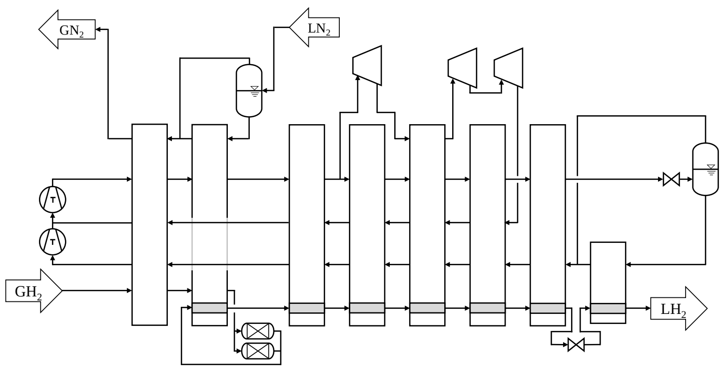

Figure 2: Flowsheet of the selected 5 tpd plant based on OHLIG & DECKER 2024 [5]

It deploys a hydrogen Claude cycle for refrigeration incorporating three turbo expanders, a Joule-Thomson valve, and two compression units with two piston compression stages each. Precooling from ambient temperatures to roughly 80 K is achieved using LN_2, which is released to the environment after use. Downstream of the cryogenic purification, all heat exchanger channels in the process stream are filled with catalyst to facilitate the ortho-para conversion. While eight heat exchanger sections are shown in Figure 2, it is assumed for the economic assessment that every two sections can be combined into one unit, resulting in a total of four actual heat exchangers.

For comparison, the conceptual large scale-plant by CARDELLA 2018 [4] shown in Figure 3 was selected. This plant has a liquefaction capacity of 100 tpd and features a similar setup to the selected 5 tpd plant, including a hydrogen Claude cycle with two multi-stage piston compression units and a total of seven turbo expanders. However, instead of open-loop precooling with LN_2, it employs a closed-loop mixed refrigerant (MR) cycle to cool the hydrogen gas from ambient temperature to approximately 100 K. The MR composition, as specified in [4], is: 14% nitrogen, 30% methane, 25% i-butane, 31% ethane. Using MR allows closer temperature profiles in the precooling section while allowing the use of standard equipment from liquefied natural gas (LNG) applications. Still, in contrast to the open precooling cycle in Figure 2, additional equipment is required, including turbo compressors, phase separators, and a pump.

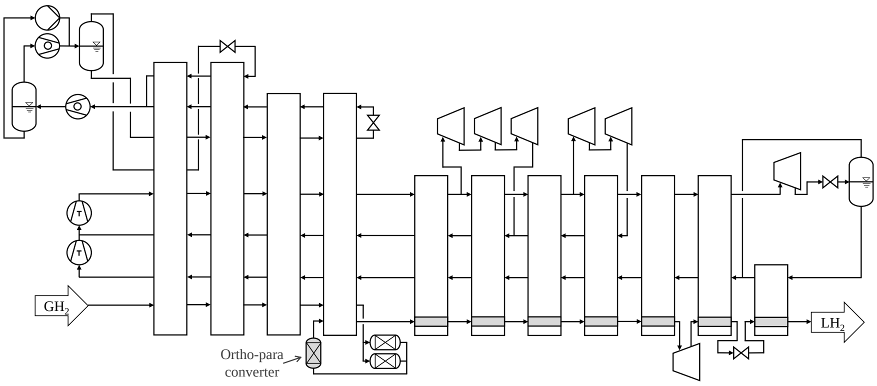

Figure 3: Flowsheet of the selected 100 tpd plant based on Cardella 2018 [4]

Additionally to the continuous ortho-para conversion within the heat exchangers of the cryogenic section, the 100 tpd plant also applies a batch ortho-para converter after precooling. While the original design by [4] includes only three actual heat exchangers, the schematic representation shown here splits these into individual sections for clarity. For the economic assessment, however, it is assumed that these sections are recombined into three total heat exchangers.

The selected flowsheets are simulated in UniSim® Design using Refprop [6] which deploys the equation of state by Leachman et al. 2009 [7] for ortho- and parahydrogen. The plants are designed to achieve minimum temperature differences of 1 K to 3 K in the heat exchangers. Furthermore, the adsorption is considered only by means of a slight temperature increase of 0.2 K and a pressure drop of 0.1 bar, while pre compression and pre purification are neglected. For the turbo expanders, an isentropic efficiency of 85% is assumed. Regarding the compressors, the isentropic efficiency is set to 70% for today's 5 tpd plant and to 80% for the conceptual 100 tpd plant. The thermodynamic states of the GH_2 feed and the LH_2 product are specified in Table 1, in accordance to [4].

Table 1: Thermodynamic states of the feed and the product of the considered plants

	5 tpd plant	100 tpd plant
Feed temperature	303 K	295 K
Feed pressure	24 bar	25 bar
Feed parahydrogen fraction	25%	25%
Product temperature	21 K	22.5 K
Product pressure	1.3 bar	2 bar
Product parahydrogen fraction	99.45%	99.13%

2.2 Simulation of the Ortho-Para Conversion

This paper places special focus on the simulation of the ortho-para conversion. Hydrogen is mixture of its ortho and para form which differ in nuclear spin. At room temperature, an equilibrium composition of 25% para and 75% orthohydrogen is observed. When the temperature decreases, the equilibrium shifts towards parahydrogen and at typical liquid hydrogen temperatures, almost only parahydrogen remains. Thus, a conversion of ortho- to parahydrogen occurs due to the hydrogen liquefaction process. [7]

This conversion would happen by itself within a few days or weeks [8]. However, since the conversion process generates heat, it would be unfavorable for it to occur within LH_2 storage tanks, as it would evaporate parts of the stored LH_2. Therefore, the conversion of ortho- to parahydrogen is facilitated to occur continuously within the hydrogen liquefaction plant using catalyst-filled heat exchangers.

For reliable results, the conversion and the associated heat must be realistically integrated into the simulation. However, REFPROP [6], which is used for property data, does not feature equilibrium hydrogen. Instead, the hydrogen process stream is defined as a mixture of ortho- and parahydrogen. Thus, a workaround for the calculation of the ortho-para conversion while using REFPROP [6], as suggested by KANZ ET AL. 2025 [9], is applied in this paper. Thereby, first, the equilibrium composition of hydrogen is calculated with the following equation, using the parameters a_1 to a_6 given in [9].

$$K_{\text{eq}}(T) = \frac{y_{\text{para}}}{y_{\text{ortho}}} = \frac{1 + 5\mathrm{e}^{-a_1/T} + 9\mathrm{e}^{-a_2/T} + 13\mathrm{e}^{-a_3/T}}{9\mathrm{e}^{-a_4/T} + 21\mathrm{e}^{-a_5/T} + 48\mathrm{e}^{-a_6/T}} \tag{1}$$

Then, the associated molar heat of conversion $\Delta h_{\text{C}}(T)$ is determined using the van't Hoff relation in Equation (2) and the derivative of Equation (1). The molar heat of conversion is defined as $\Delta h_{\text{C}} = -\Delta h^0_{\text{R}}(T)$. A detailed derivation of this approach is given in KANZ ET AL. 2025 [9].

$$\frac{\partial \ln K_{\text{eq}}(T)}{\partial T} = \frac{\Delta h^0_{\text{R}}(T)}{RT^2} \tag{2}$$

For integration into the simulation in UniSim® Design, these calculations take place within spreadsheets. It is assumed that the hydrogen composition is always lagging 2 K behind the equilibrium due to conversion kinetics. While the hydrogen's composition is overwritten with the new composition after the considered heat exchanger, the heat is not applied punctually. Instead, it is applied throughout the heat exchanger, using an additional virtual stream having the thermodynamic state of the considered hydrogen process stream. The virtual stream is led through the heat exchanger while delivering the heat calculated in the spreadsheet. This allows precise allocation of the conversion heat to the hot composites throughout the heat exchanger.

2.3 Techno-Economic Modeling

The results of the process simulation are used for assessing the plants techno-economically by estimating capital expenditures (CAPEX) and operational expenditures (OPEX). For the CAPEX, the factor based model by TURTON ET AL. 2018 [10] is applied. It uses factors to scale costs based on equipment size, type, and material, utilizing data from historical cost records and industry standards. Further, it accounts for installation, indirect expenses, contingencies, fees, and auxiliaries. When the size of a component exceeds the range given in [10], the costs are scaled using the cost-scaling function by COUPER 2003 [11].

For estimation of a plant's OPEX, the power consumption resulting from the simulation is used, with an electricity price of 50 USD/MWh which roughly correlates to power generation costs from renewable energy [12]. The power consumption is divided into two categories: the plant's own power consumption and the power consumption for the precoolant. For precooling with MR, this corresponds to the power consumption within the MR cycle. For LN_2 precooling, a specific power consumption of $0.5\,\text{kWh/kg}_{\text{LN}_2}$ [4] is assumed which relates to LN_2 production in air separation units [13]. In addition, operation and maintenance (O&M) costs contribute to the OPEX. A constant annual O&M factor of 5% of the CAPEX is chosen, which is a typical value for chemical plants [14]. All costs shown in this paper are calculated in 2023 USD, using the Chemical Engineering Plant Cost Index (CEPCI) [15]. The simulated plants include storage capacities of 5 and 2 days, respectively. For the 5 tpd plant, a larger storage was chosen as smaller plants typically need more buffer for irregular demand. Further assumptions of the techno-economic model are summarized in Table 2.

For the techno-economic analysis, three key parameters are considered: the specific CAPEX relates the overall CAPEX to the mass flow rate of liquefied hydrogen.

$$\text{Spec. CAPEX} = \frac{\text{CAPEX}}{\dot{M}_{\text{LH}_2}} \tag{3}$$

The specific energy consumption (SEC) is the net power of the plant per mass flow rate of liquefied hydrogen. The net power thereby results from the power P_{required} required for compression of the refrigerant and for the precoolant, and from the power $P_{\text{recovered}}$ that can be recovered in the turbo expanders. However, recovering the power in the turbo expanders has only a small effect in the magnitude of 5% on the SEC [4].

$$\text{SEC} = \frac{P_{\text{required}} - P_{\text{recovered}}}{\dot{M}_{\text{LH}_2}} \tag{4}$$

Finally, the specific liquefaction cost (SLC) relates the annual OPEX and the annual share of the CAPEX (CAPEX_a) to the mass flow rate of liquefied hydrogen. Thereby, the SLC is just the specific cost of liquefaction and not of liquid hydrogen, as no supply chain costs are involved.

$$\text{SLC} = \frac{\text{CAPEX}_a + \text{OPEX}}{\dot{M}_{\text{LH}_2}} \tag{5}$$

Table 2: Techno-economic assumptions

O&M factor	5% of CAPEX
Electricity price	50 USD/MWh
Specific energy consumption for LN_2	$0.5\,\mathrm{kWh/kg_{LN_2}}$
Exchange rate	$1\,€ = 1.05\,\mathrm{USD}$
Depreciation period	20 years
Plant utilization rate	95%
Interest rate	7%
Hydrogen loss	1%
Auxiliary power consumption	3% of net power
Turbine energy recovery efficiency	80%
Storage capacity	2 days (100 tpd) and 5 days (5 tpd plant)
Insulation	20% of vessel cost
Pipes, valves, cooling water, etc.	Neglected for economics

3 Results

The SLC of both plants, calculated from the process simulation results and the techno-economic model, is shown in Figure 4(a). To give a clearer picture, pie charts in Figures 4(b) to 4(e) break down the contributions of the individual components of OPEX and CAPEX.

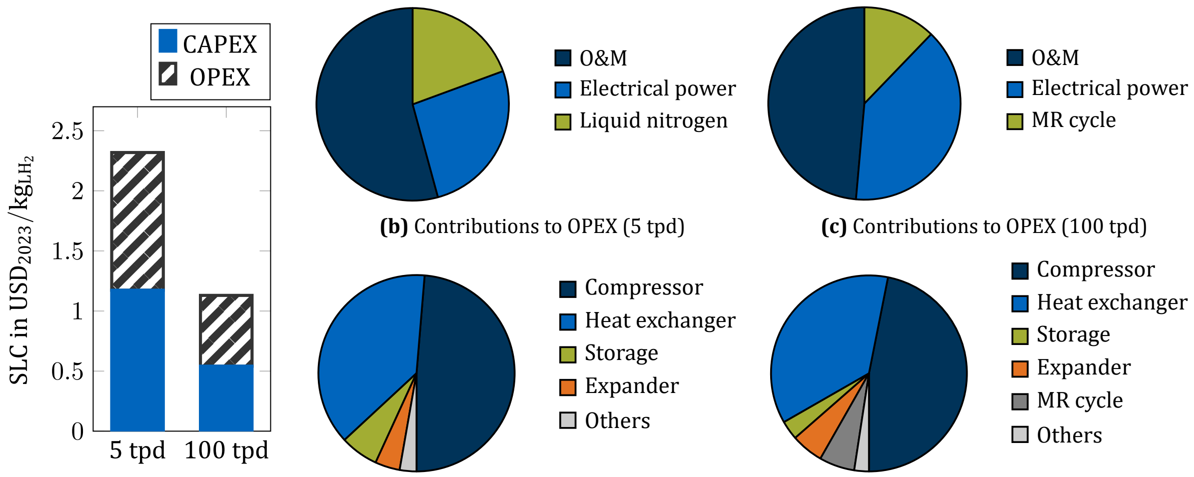

(a) SLC of both plants **(b)** Contributions to OPEX (5 tpd) **(c)** Contributions to OPEX (100 tpd) **(d)** Contributions to CAPEX (5 tpd) **(e)** Contributions to CAPEX (100 tpd)

Figure 4: Techno-economic results: specific liquefaction costs (SLC) and individual contributions to OPEX and CAPEX of both considered plants

Figure 4(a) highlights the shares of OPEX and CAPEX in the overall SLC, indicating that both contribute equally in both plants. Additionally, the techno-economic analysis reveals that the SLC is roughly halved in the large-scale plant compared to the smaller-scale plant due to economy of scale.

In Figure 5, the specific CAPEX of the considered plants is plotted against plant size and compared to literature values normalized to 2023 USD. To explore the scalability of even larger plants, a 200 tpd plant was additionally simulated by scaling up the 100 tpd design. In doing so, the maximum equipment sizes, particularly for compressors and heat exchangers, were constrained according to the limits defined in [4]. The results align well with the literature range, showing a significant reduction of the specific CAPEX with plant size. However, at plant sizes beyond 100 tpd the influence of economy of scale is small, which is partly due to the limited scalability of key components as hydrogen piston compressors [4].

The results for the SEC, as shown in Figure 6, also fall within the range reported in the literature. However, the results of this study have a rather low energy consumption. A significant decrease of the SEC with plant size is evident. Thereby, the reduction in SEC between the 5 tpd and the 100 tpd plant is not solely due to

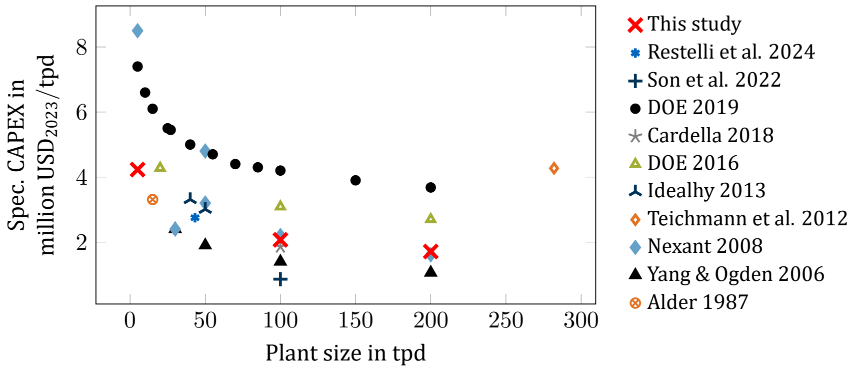

Figure 5: Comparison of this study's results regarding the specific CAPEX depending on the plant size with literature data [1, 4, 16–24]

economy of scale; differences in the precooling process also play a vital role. Consequently, when going to the even larger 200 tpd plant, only minor further reduction is achieved.

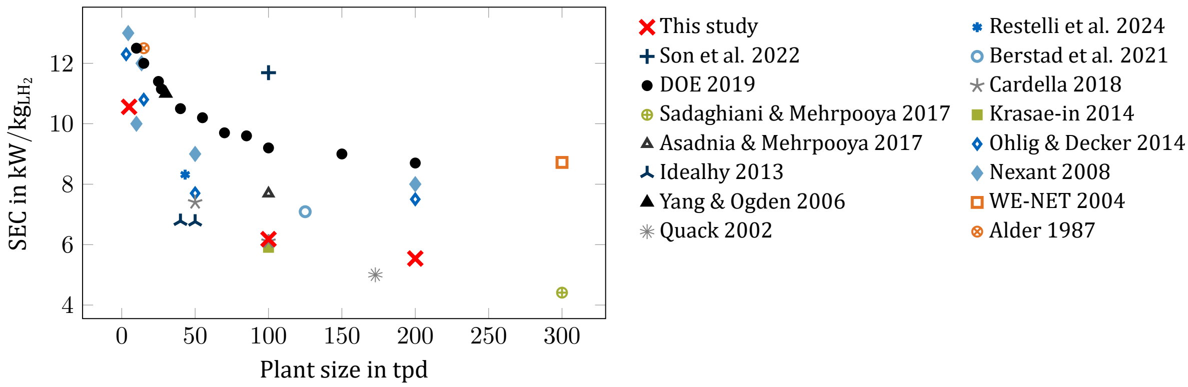

Figure 6: Comparison of this study's results regarding the specific energy consumption SEC depending on the plant size with literature data [1, 4, 5, 16–18, 20, 22–30]

A closer investigation of the individual contributions to OPEX and CAPEX of the 5 tpd and the 100 tpd plant in Figure 4 shows that the CAPEX (Figure 4(d) and Figure 4(e)) is dominated by the compressors and heat exchangers while all other components have minor influence. Even though in the 100 tpd plant, additional equipment is required for the closed MR cycle, it does not add up significantly to the CAPEX. Considering the OPEX (Figure 4(b) and Figure 4(c)), the largest share in both cases is O&M costs, driven by a high CAPEX and the assumption, that annual O&M costs equal 5% of the CAPEX. The other considered contributions to the OPEX are electrical power consumption. Costs associated with LN_2 in the 5 tpd plant and with the MR cycle in the 100 tpd plant, respectively, are allocated to precooling and considered separately from the plant's remaining electrical power consumption. Notably, the share of the OPEX allocated to the precooling drops significantly in the large-scale plant with MR.

However, in both figures, the O&M costs are significantly high which leads to the conclusion that the typical O&M factor from the literature overestimates the costs. Considering that a hydrogen liquefaction plant is a rather simple plant without reaction or corrosive fluids and with a relatively small amount of moving parts, one could assume lower O&M costs. Thus, to show the high influence of the assumptions, two sensitivity studies are conducted for the 100 tpd plant. First, the techno-economical analysis is repeated, assuming an annual O&M factor of only 2% of the CAPEX but maintaining all other assumptions (adaption A). Then, additional assumptions are altered for a second case (adaption B), representing typical "today's" conditions. The depreciation period is reduced to 10 years, which aligns with the typical contract duration for gas supply agreements. Further, 3 years of planning and construction are considered, where capital expenses are incurred before operation, which has been neglected so far.

The results of adaption A and B are shown in Figure 7, where Figure 7(a) displays the SLC of the adaptions alongside the reference case. While adaption A has a slightly smaller SLC due to a smaller OPEX, adaption B results in a larger SLC. Additionally, in adaption B, CAPEX dominates the overall costs, mainly resulting from the shorter depreciation period. Further, Figure 7(c) shows the individual contributions to the OPEX for both adaptions in comparison to the reference case in Figure 7(b). A high dependency on the O&M assumption is concluded. No comparison of the CAPEX distribution is shown as this was not altered by the case study.

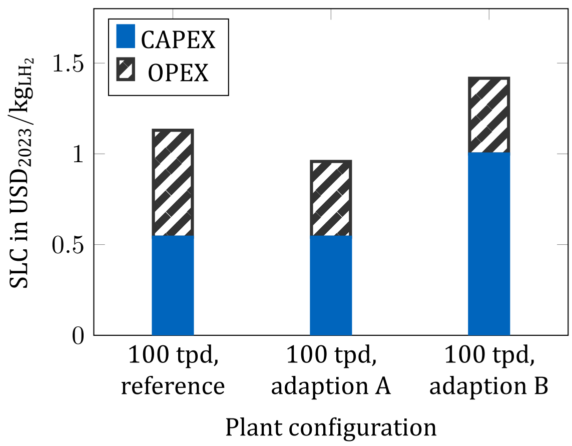

(a) SLC of the 100 tpd reference case and both adaptions

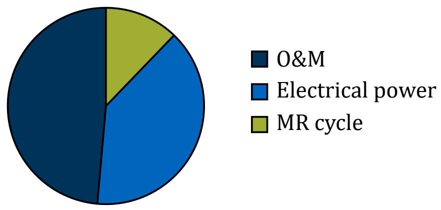

(b) Contributors to OPEX (100 tpd, reference case)

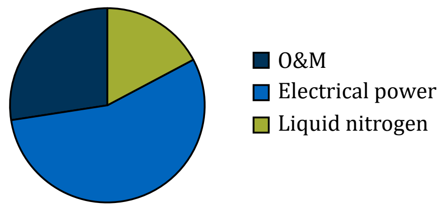

(c) Contributors to OPEX (100 tpd, adaptions A and B)

Figure 7: Techno-economic results: specific liquefaction costs (SLC) and individual contributors to OPEX of the adaptions and the reference case (100 tpd).

4 Conclusion

This paper has provided techno-economic results for hydrogen liquefaction plants based on comprehensive process simulations in UniSim® Design with integrated ortho-para conversion using the approach by Kanz et al. 2025 [9]. The results indicate equal contribution of CAPEX and OPEX to the overall costs and show good agreement with the literature. Further, the costs can be significantly reduced when building large-scale hydrogen liquefaction plants. Closer examination of individual contributions to CAPEX and OPEX identify compressors and heat exchangers as main cost drivers and indicate a high dependency on the study's assumptions for O&M costs. Thus, further case studies with adaptions regarding the O&M factor, depreciation period, and construction period have been conducted.

While future LH_2 demands require building large-scale liquefaction plants, these must also be integrated into cost-efficient large-scale supply networks, which requires highly optimized distribution routes. As LH_2 infrastructure is expected to significantly impact overall costs, this should be investigated in future work.

Acknowledgments

The authors gratefully acknowledge the financial support of the joint project "HyNEAT" by the German Federal Ministry of Education and Research (BMBF, FKZ 03SF0670F) and the project supervision by the project management organization Projektträger Jülich (PtJ).

References

[1] Hoelzen J, Koenemann L, Kistner L, Schenke F, Bensmann A and Hanke-Rauschenbach R 2023 H2-powered aviation – design and economics of green LH2 supply for airports *Energy Convers. Manag.: X* 20 100442 https://doi.org/10.1016/j.ecmx.2023.100442

[2] Zhang T, Uratani J, Huang Y, Xu L and Griffiths S 2023 Hydrogen liquefaction and storage: Recent progress and perspectives *Renew. Sustain. Energy Rev.* 176 113204 https://doi.org/10.1016/j.rser.2023.113204

[3] Oesingmann K, Grimme W and Scheelhaase J 2004 Hydrogen in aviation: A simulation of demand, price dynamics, and CO2 emission reduction potentials *Int. J. Hydrog. Energy* 64 633–642 https://doi.org/10.1016/j.ijhydene.2024.03.241

[4] Cardella U F 2018 *Large-scale hydrogen liquefaction under the aspect of economic viability* Dissertation Technical University of Munich
[5] Ohlig K and Decker L 2014 The latest developments and outlook for hydrogen liquefaction technology *AIP Conf. Proc.* pp 1311–1317
[6] Lemmon E W, Bell I H, Huber M L and McLinden M O Nist reference fluid thermodynamic and transport properties database (refprop) version 10 - srd 23
[7] Leachman J W, Jacobsen R T, Penoncello S G and Lemmon E W 2009 Fundamental equations of state for parahydrogen, normal hydrogen, and orthohydrogen *J. Phys. Chem. Ref. Data* 38 721–748 https://doi.org/10.1063/1.3160306
[8] Al Ghafri et al 2022 Hydrogen liquefaction: a review of the fundamental physics, engineering practice and future opportunities *Energy Environ. Sci.* 15 2690–2731 https://doi.org/10.1039/D2EE00099G
[9] Kanz B, Tafone A, Stops L, Massier T and Klein H 2025 A novel approach to simulate ortho-para conversion in hydrogen liquefaction based on the van't Hoff equation *Int. J. Hydrog. Energy* https://doi.org/10.1016/j.ijhydene.2025.02.304
[10] Turton R 2018 *Analysis, synthesis, and design of chemical processes* 5th ed (Boston: Prentice Hall) ISBN 9780134177403
[11] Couper J R 2003 *Process engineering economics* (New York, NY: Dekker) ISBN 0-8247-4036-X
[12] International Renewable Energy Agency (IRENA) Renewable power generation costs in 2024
[13] Bracha M and Decker L 2008 Grosstechnische Wasserstoffverfluessigung in Leuna *Deutsche Kaelte-Klima-Tagung*
[14] Peters M S, Timmerhaus K D and West R E 2003 *Plant design and economics for chemical engineers* 5th ed (Boston: McGraw-Hill) ISBN 978-0071198721
[15] Chemical Engineering 2025 The chemical engineering plant cost index URL `https://www.chemengonline.com/pci-home`
[16] Restelli F, Spatolisano E, Pellegrini L A, Cattaneo S, de Angelis A R, Lainati A and Roccaro E 2024 Liquefied hydrogen value chain: A detailed techno-economic evaluation for its application in the industrial and mobility sectors *Int. J. Hydrog. Energy* 52 454–466 https://doi.org/10.1016/j.ijhydene.2023.10.107
[17] Son H, Yu T, Hwang J and Lim Y 2022 Simulation methodology for hydrogen liquefaction process design considering hydrogen characteristics *Int. J. Hydrog. Energy* 47 25662–25678 https://doi.org/10.1016/j.ijhydene.2022.05.293
[18] Conelly E, Penev M, Elgowainy A and Hunter C DOE hydrogen and fuel cells program record: Current status of hydrogen liquefaction costs
[19] Reddi K, Elgowainy A and Brown D DOE hydrogen fuel cells program annual merit review: Hydrogen delivery infrastructure analysis
[20] Stolzenburg K and Mubbala R Integrated design for demonstration of efficient liquefaction of hydrogen (IDEALHY): Hydrogen liquefaction report
[21] Teichmann D, Arlt W and Wasserscheid P 2012 Liquid Organic Hydrogen Carriers as an efficient vector for the transport and storage of renewable energy *Int. J. Hydrog. Energy* 37 18118–18132 https://doi.org/10.1016/j.ijhydene.2012.08.066
[22] Nexant Inc, Air Liquide, Argonne National Laboratory, Chevron Technology Venture, Gas Technology Institute, National Renewable Energy Laboratory, Pacific Northwest National Laboratory and TIAX LLC 2H2A hydrogen delivery infrastructure analysis models and conventional pathway options analysis results: Interim report
[23] Yang C and Ogden J 2007 Determining the lowest-cost hydrogen delivery mode *Int. J. Hydrog. Energy* 32 268–286 https://doi.org/10.1016/j.ijhydene.2006.05.009
[24] Swiss Group 1987 Hydrogen in air transportation. Feasibility study for Zurich airport, Switzerland *Int. J. Hydrog. Energy* 12 571–585
[25] Berstad D, Skaugen G and Wilhelmsen Ø 2021 Dissecting the exergy balance of a hydrogen liquefier: Analysis of a scaled-up claude hydrogen liquefier with mixed refrigerant pre-cooling *Int. J. Hydrog. Energy* 46 8014–8029 https://doi.org/10.1016/j.ijhydene.2020.09.188
[26] Sadaghiani M S and Mehrpooya M 2017 Introducing and energy analysis of a novel cryogenic hydrogen liquefaction process configuration *Int. J. Hydrog. Energy* 42 6033–6050 https://doi.org/10.1016/j.ijhydene.2017.01.136
[27] Asadnia M and Mehrpooya M 2017 A novel hydrogen liquefaction process configuration with combined mixed refrigerant systems *Int. J. Hydrog. Energy* 42 15564–15585 https://doi.org/10.1016/j.ijhydene.2017.04.260
[28] Krasae-in S 2014 Optimal operation of a large-scale liquid hydrogen plant utilizing mixed fluid refrigeration system *Int. J. Hydrog. Energy* 39 7015–7029 https://doi.org/10.1016/j.ijhydene.2014.02.046
[29] Ohira K 2004 A summary of liquid hydrogen and cryogenic technologies in japan's WE-NET project *AIP Conf. Proc.* pp 27–34
[30] Quack H 2002 Conceptual design of a high efficiency large capacity hydrogen liquefier *AIP Conf. Proc.* pp 255–263